Water splitting by electrolysis at high current density under 1.6 volt

Journal:	*Energy & Environmental Science*
Manuscript ID	EE-ART-03-2018-000927.R1
Article Type:	Paper
Date Submitted by the Author:	17-May-2018

Complete List of Authors:	Zhou, Haiqing; University of Houston, Department of Physics; Hunan Normal University, Physics and Electronics Yu, Fang; University of Houston, Department of Physics and TcSUH; Hunan Normal University, Physics and Electronics Zhu, Qing; University of Houston Sun, Jingying; University of Houston, Physics Qin, Fan; University of HOUSTON, Department of Electrical and Computer Engineering Luo, Yu; Central China Normal University, Bao, Jiming; University of Houston, Department of Electrical and Computer Engineering Yu, Ying; Central China Normal University, Institute of Nanoscience and Nanotechnology Chen, Shuo; University of Houston, Physics Ren, Zhifeng ; University of Houston, Physics

Energy & Environmental Science

Paper

Water splitting by electrolysis at high current density under 1.6 volt

Haiqing Zhou,[†a,b] Fang Yu,[†a,b] Qing Zhu,[a] Jingying Sun,[a] Fan Qin,[d] Luo Yu,[c] Jiming Bao,[d] Ying Yu,*[c] Shuo Chen*[a] and Zhifeng Ren*[a]

Received 00th January 20xx,
Accepted 00th January 20xx

DOI: 10.1039/x0xx00000x

www.rsc.org/

Splitting water into hydrogen and oxygen by electrolysis using electricity from intermittent waste heat, wind, or solar energies is one of the easiest and cleanest methods for high-purity hydrogen production and an effective way to store the excess electrical power. The key dilemma for efficient large-scale production of hydrogen by splitting of water via hydrogen and oxygen evolution reactions (HER and OER, respectively) is the high overpotential required, especially for OER. We report an exceptionally active and durable OER catalyst yielding current densities of 500 and 1,000 mA cm^{-2} at overpotentials of only 259 mV and 289 mV in alkaline electrolyte, respectively, fulfilling the commercial criteria of the OER process. Together with a good HER catalyst, we have achieved the commercially required current densities of 500 and 1,000 mA cm^{-2} at 1.586 and 1.657 V, respectively, with very good stability, dramatically lower than any previously reported voltage. This discovery sets the stage for large-scale hydrogen production by water splitting using the excess electrical power whenever and wherever available.

Broader context

Water electrolysis for hydrogen production is one of the easiest and cleanest routes to store the considerable intermittent clean energy resources (wind, waste heat, solar, etc) on a large scale. At present, mass production in industry remains challenging (< 5%) due to the high cost of noble metals as catalysts in acid and low energy conversion efficiency of non-noble metal catalysts in base. Although many water electrolyzers have been constructed experimentally by designing robust electrocatalysts, most of them still need cell voltages significantly larger than 1.8 V to deliver 200 mA cm^{-2}, unsatisfactory for the commercial requirements. Especially, for H_2 to play an important role in the energy sector, water splitting at current density ≥ 500 mA cm^{-2} under 1.6 V is required, in which the OER is the main bottleneck with poor efficiency. Here we develop a straightforward room-temperature strategy to fabricate a robust and durable OER catalyst yielding 500 and 1,000 mA cm^{-2} at low overpotentials in alkaline electrolyte, fulfilling the commercial criteria of the OER process. Integrating it into a water electrolyzer can realize the commercially electrolysis current of 500 and 1,000 mA cm^{-2} at around 1,6 V with excellent durability. This discovery is an advanced development toward large-scale H_2 production using the excess electrical power whenever and wherever available.

Increasing the fraction of clean energy over fossil fuels including coal, petroleum, and natural gas will certainly reduce pollution,[1] but large-scale utilization of the considerable intermittent clean energy resources, such as wind, wave power, waste heat, and solar energies, requires reliable storage of electrical power, and the same applies to the oversupply of the electrical power from sources such as nuclear power plants during the night. Hydrogen is a good energy carrier for energy storage. Water electrolyzers are promising commercial apparatus to produce high-purity hydrogen with unlimited water resources, among which alkaline water electrolyzers are more appealing than that based on proton exchange membrane (PEM) in acid.[2,3] This is primarily because low-cost electrocatalysts, instead of noble metal-based catalysts, can be utilized in alkaline media. However, efficient and mass hydrogen production in industry has not been widely deployed at present (< 5% hydrogen production) due to the high cost of the noble metals as catalysts in acid and the low energy conversion efficiency of the non-noble metal catalysts in base. Although a variety of alkaline water electrolyzers have been constructed by designing robust electrocatalysts,[3-5] most of them require cell voltages significantly larger than 1.8 V to deliver 200 mA cm^{-2}, unsatisfactory for the commercial requirements of 1.8-2.4 V for current densities of 200-400 mA cm^{-2}. In particular, the key challenge is to employ the overall water splitting durably at high current densities above 500 mA cm^{-2}. Thus, it is of high desire to develop robust electrocatalysts to substantially expedite the strongly uphill water splitting process[6-8] and to maintain the activity at high current densities, so as to greatly improve the electrolysis efficiency for large-scale water splitting.

[a]*Department of Physics and TcSUH, University of Houston, Houston, TX 77204, United States. Email: schen34@uh.edu, zren@uh.edu*
[b]*School of Physics and Electronics, Hunan Normal University, Changsha 410081, China.*
[c]*College of Physical Science and Technology, Central China Normal University, Wuhan 430079, China. Email: yuying01@mail.ccnu.edu.cn*
[d]*Department of Electrical and Computer Engineering, University of Houston, Houston, TX 77204, United States*
[†]*These authors contributed equally to this work.*
†Electronic Supplementary Information (ESI) available: experimental details and results. See DOI: 10.1039/x0xx00000x

Essential to the full water splitting reaction is the half reaction called oxygen evolution reaction (OER), which is the bottleneck due to the sluggish kinetics arising from the rigid O-O double bond formation and the multiproton-coupled electron transfer steps.[9-11] Although substantial advancements have been accomplished in the development of robust OER catalysts, neither the benchmark noble IrO_2 and RuO_2 catalysts,[12] nor the non-precious OER electrocatalysts, including transition metal oxides,[5,12,13] nitrides,[14] selenides,[15] phosphides,[16] and phosphate,[17,18] are effective enough for efficient anodic OER. Especially, very few catalysts can satisfy the strict industrial criteria that the OER process should be energetically catalyzed over a long period at extremely high current densities ($\geqslant$ 500 mA cm^{-2}) with overpotentials $\leqslant$ 300 mV,[10,17] which hinders the widespread implementation of these available electrocatalysts. It is noted that iron metaphosphate is the only OER catalyst satisfying the strict criteria,[17] however, the preparation method is complicated, not environmentally friendly and safe, since toxic PH_3 was involved. Especially, the stability of this catalyst operated at high current density 500 mA cm^{-2} was still not satisfactory, not to mention at even higher current densities. Aiming at commercially practical high-performing and environmentally friendly OER catalysts, we report an outstanding oxygen-evolving electrocatalyst constructed by three-dimensional porous interwoven (Ni,Fe) oxyhydroxide nanorod arrays, which are mainly derived from amorphous Ni/Fe (oxy)hydroxide mesoporous films on Ni foams synthesized by a simple yet industrially compatible strategy based on room-temperature mechanical stirring. Then an outstanding alkaline water electrolyzer was constructed by pairing this OER catalyst with another robust $MoNi_4$ catalyst for the HER, which exhibits a record low voltage of about 1.6 V for efficient overall-water-splitting activity and can be driven by different power sources, such as an AA battery or a commercial thermoelectric power generator.

The key in pursuing efficient OER electrocatalysts is to design catalysts with large surface area and high-density active sites directly grown on three-dimensional conductive porous scaffolds,[19-21] so that multiple levels of porosity with high-density active sites and good conductivity can be simultaneously integrated in the same device. Here we employed commercial Ni foams as the conductive support,[22] and synthesized amorphous mesoporous Ni/Fe (oxy)hydroxide [(Ni,Fe)OOH] film on their surface by room-temperature mechanical stirring processing, which is normally used for preparing amorphous FeOOH for use in supercapacitors.[23] Different from this conventional process, we creatively introduced a new chemical reaction between metallic Ni and $FeCl_3$ during mechanical stirring, and synthesized amorphous FeOOH and $Ni(OH)_2$ simultaneously, which is further evolved into a robust OER electrocatalyst during electrocatalysis as discussed below. This approach is very simple yet effective not involving in any complicated procedures or poisonous chemicals relative to other growth procedures for preparing efficient OER catalysts, and is also different from traditional methods for preparing OER catalyst by means of electrodeposition or hydrothermal synthesis of transition metal Ni/Fe oxides on Ni foam, since Ni foam used here was etched and reacted with the solution to form $Ni(OH)_2$ particles simultaneously.

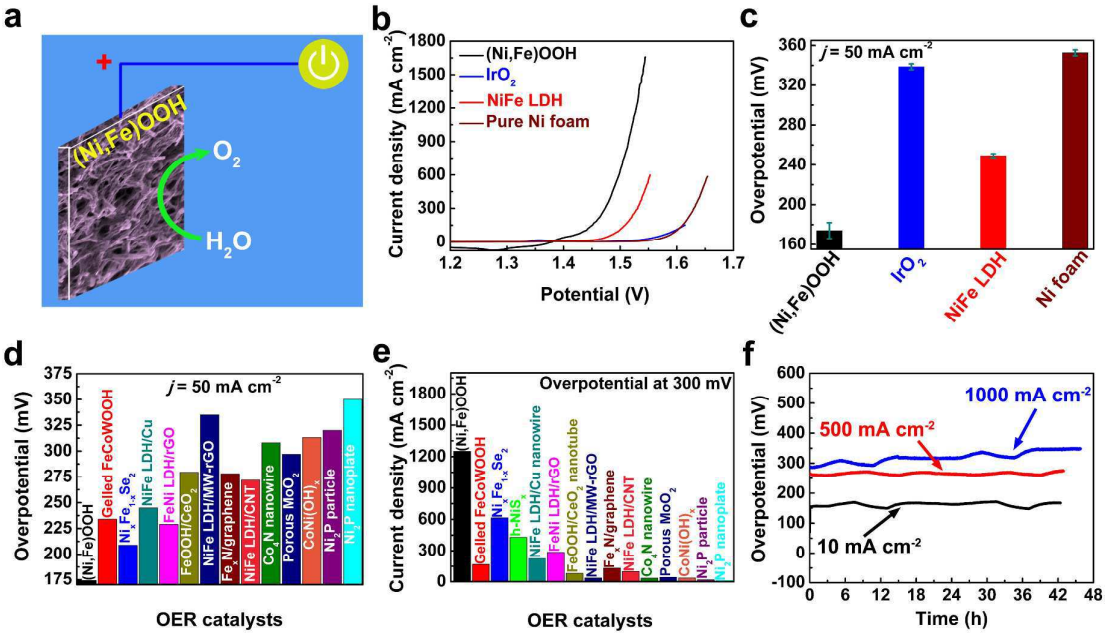

Fig. 1. Electrocatalytic water oxidation. (a) Schematic diagram of the Ni/Fe (oxy)hydroxide nanostructures supported on Ni foam for water oxidation in 1 M KOH. (b) Polarization curves; (c) Overpotentials required at 50 mA cm^{-2} recorded on different electrodes. The error bar shows the range of the values determined by three independent measurements. (d) Comparison of the overpotentials at 50 mA cm^{-2} between this catalyst and other reported robust OER electrocatalysts. (e) Comparison of the current densities at overpotential of 300 mV between this catalyst and other available robust OER electrocatalysts. (f) Chronoamperometric measurements of the water oxidation reaction at 10, 500, and 1,000 mA cm^{-2} on the Ni/Fe electrode, suggesting good durability when operated at high current density, which meets the strict criterion for commercial utilization.

After growth, deionized water cleaning and drying in air overnight are all that is required, and the as-prepared multi-porous catalysts were then directly utilized as a self-supported anode for water oxidation reaction (Fig. 1a) using a three-electrode configuration in 1M KOH as reported previously.[14,17] For comparison, a bare Ni foam, NiFe layered double hydroxide (LDH) nanosheets (Fig. S1, ESI†), and the benchmark IrO_2 catalysts on a Ni foam were also included here. Apparently, as revealed in Fig. 1b, this amorphous (Ni,Fe)OOH electrode exhibited significantly enhanced catalytic OER activity. It requires an overpotential as low as 174 mV to achieve a current density of 50 mA cm^{-2} (Fig. 1c), which is 75, 165, and 179 mV less than the state-of-the-art NiFe nanosheets/Ni foam (249 mV), the benchmark IrO2 electrode (339 mV), and the Ni foam (353 mV), respectively. This overpotential is also substantially lower than that of any of the non-precious OER catalysts (Fig. 1d, Table S1, ESI†) including recently reported excellent electrocatalysts $Fe(PO_3)_2$-derived oxyhydroxide (213 mV),[17] G-FeCoW oxyhydroxide/gold foam (234 mV),[13] $Ni_xFe_{1-x}Se_2$-derived hydroxide nanosheets (209 mV),[15] and NiFe LDH/graphene (335 mV),[24] and so forth. At the overpotential of 300 mV, this catalyst can deliver a current density up to 1,251 mA cm^{-2} (Fig. 1e, Table S1, ESI†). In particular, our OER catalyst requires overpotentials of only 259 and 289 mV to achieve 500 and 1000 mA cm^{-2}, respectively (Table S1, ESI†). The outstanding catalytic behavior toward water oxidation is primarily due to the amorphous (Ni,Fe)OOH film, rather than the Ni foam support.

The operating durability is another essential performance index to assess the application in catalysis. To characterize the performance stability of this OER catalyst, we ran water oxidation continuously under constant current densities (Fig. 1f). Notably, this catalyst withstood accelerated degradation tests, and the overpotential needed to reach a current density of 10 mA cm^{-2} varies very little at 154 mV for over 42 h, corroborating that the catalytic activity can be sustained upon OER testing. For applications, the catalyst must survive over a long period at high-current operation conditions (≥ 500 mA cm^{-2}).[10,17] This catalyst also shows sustainable capability of being operated continuously at 500 and 1,000 mA cm^{-2} over 44 h with no significant decay (Overpotentials increase by merely 11 mV, 14 mV and 59 mV for current densities of 10, 500 and 1000 mA cm^{-2} after 44h electrolysis), as revealed in Fig. 1f, verifying its durability during OER electrocatalysis, which is far better than the previously reported $Fe(PO_3)_2$-derived catalyst[17] with higher catalyst loading and NiFe LDH/Cu nanowire arrays (Fig. S2, ESI†).[25] The long-term robustness is probably attributed to the absence of polymer binder and to the strong interconnection between the topmost catalyst and the Ni foam support. To the best of our knowledge, this catalyst is adequate to fulfil the aforementioned strict criteria (low voltage for high current density) toward commercial utilization of alkaline water electrolyzers, outperforming most non-noble OER catalysts reported thus far, as well as the benchmark precious IrO_2 catalysts. Although Ni/Fe (oxy)hydroxides are well known as promising OER electrocatalysts, most of the reported electrocatalysts, specifically the best one from NiFe LDH/rGO,[26] still require 229 mV overpotentials to reach 50 mA cm^{-2}. In particular, there are no OER electrocatalysts made of Ni/Fe oxyhydroxides reporting good durability over a long term at large current densities like 500 and 1000 mA cm^{-2}, meaning that there is no such kind of OER catalyst fulfilling the aforementioned commercial criteria. Thus, although the active sites of our OER catalysts still originate from Ni/Fe (oxy)hydroxide evolved from a mixed composite of $Ni(OH)_2$ and FeOOH, it is interesting to point out that our catalyst is the first Ni/Fe (oxy)hydroxide-based OER catalyst satisfying the commercial criteria hitherto. Especially, considering the kinds of solvent, starting materials and the procedures used here, this method may be applicable to fabricate many other catalysts for hydrogen evolution or oxygen evolution reaction, especially the latter one, including Cu-, Ni-, Fe-, or Co-based (oxy)hydroxides, but it is necessary to consider lots of factors including the species of starting materials, the kinds of solvents, the chemical reactions among different starting precursors, and the solubility of the starting materials and the as-obtained catalysts, so that the as-obtained catalyst can be strongly attached to the surface with no necessity of using the conductive polymers as the binders to fix the catalysts onto the support.

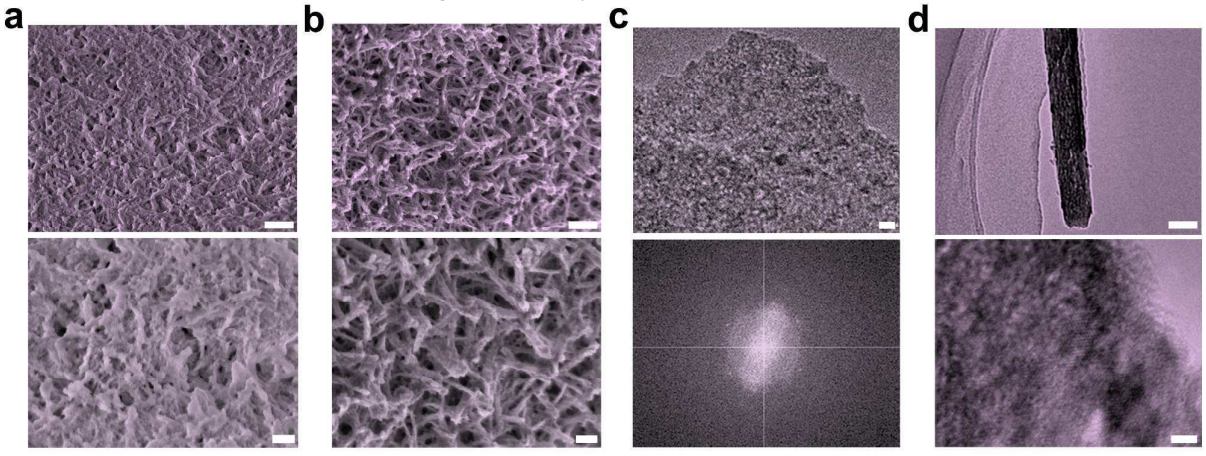

Fig. 2. Material characterization of original and post-OER catalysts by SEM and TEM. (a) Morphologies of original Ni/Fe samples. (b) Morphologies of post-OER Ni/Fe samples. (c) High-resolution TEM images of the original catalysts. (d) TEM images of the post-OER catalysts, from which we conclude that these catalysts are mainly in amorphous state. Scale bars: (a and b) 1 μm (top); 400 nm (bottom). (c) 2 nm (top). (d) 50 nm (top); 2 nm (bottom).

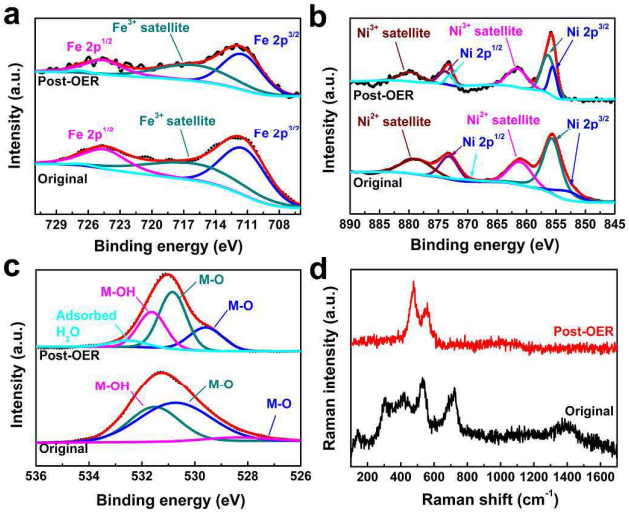

Fig. 3. XPS and Raman spectra of the original and post-OER catalysts. (a) Ni 2p XPS spectra. (b) Fe 2p XPS spectra. (c) O 1s binding energies before and after OER tests. (d) Raman spectra of the catalysts before and after OER testing.

To elucidate the possible origins of the extraordinary catalytic OER activity, we further studied the surface morphologies, surface chemical states, and composition of the (Ni,Fe)OOH electrocatalyst before and after OER tests (Fig. 2 and 3, Fig. S3, ESI†). Typical scanning electron microscopy (SEM) images of the as-prepared electrocatalysts (Fig. 2a), combined with transmission electron microscopy (TEM) (Fig. 2c), revealed that an amorphous mesoporous film is grown uniformly on the surface by mechanical stirring of Ni foam with $FeCl_3$ precursor in ethanol at room temperature.[23] This film is further confirmed to be a mixture of mainly amorphous FeOOH and $Ni(OH)_2$ by elaborate X-ray photoelectron spectroscopy (XPS) analysis (Fig. 3a-c).[23,27] The Raman frequencies appearing at 140.2, 307.7, 413.6, 534.7, 720.9, and 1395.4 cm^{-1} in the original samples (Fig. 3d) also indicated that the original samples were mainly composed of amorphous FeOOH at the surface.[27,28] The strong binding between these catalysts and Ni foams, ensuring good electrical contact and efficient charge transfer between the catalyst and current collector Ni foam, was further indicated by the low series and charge-transfer resistances from electrochemical impedance spectroscopy (EIS) (Fig. S4, ESI†). After OER testing, due to the partial dissolution of FeOOH in concentrated KOH solution,[29] the amorphous film is evolved to porous interwoven nanorod arrays, as manifested in Fig. 2b, which exposed more active sites for the OER. These arrays are confirmed to be predominantly amorphous NiOOH mixed with a small amount of FeOOH nanoparticles by high-resolution TEM image and elemental mapping (Fig. 2d, Fig. S3, ESI†), energy-dispersive X-ray spectroscopy (EDS) (Fig. S5, ESI†), XPS (Fig. 3a-c), and Raman spectrum (Fig. 3d), in which two new strong modes located at 478.6 and 556.5 cm^{-1} belonging to the Ni-O vibrations in NiOOH, rather than amorphous FeOOH,[27,30] were detected. The electrochemical double-layer capacitance (C_{dl}), estimated by a simple cyclic voltammetry method, directly manifests the electrochemically active surface area.[8,17,21] As shown in Figs. S6-S8 (ESI†), this amorphous (Ni,Fe)OOH electrode has a smaller C_{dl} value (5.9 mF cm^{-2}) compared to the NiFe LDH nanosheets/Ni foam (9.0 mF cm^{-2}), but a little larger than pristine Ni foam electrodes (5.0 mF cm^{-2}), meaning that the active surface area of this (Ni,Fe)OOH electrode has no significant difference relative to other two reference electrodes. Thus, the change of surface area cannot account for the 4.3- and 261.3-fold enhancement of its current density relative to the two reference materials, respectively, at 300 mV (Fig. 1b), unambiguously corroborating that this material has higher intrinsic catalytic activity for water oxidation.[15,17] To support this point, we roughly calculated the turnover frequencies (TOFs) at 300 mV to compare the intrinsic activities among amorphous (Ni,Fe)OOH, NiFe LDH, and IrO_2 catalysts based on the formula: TOF = $j \times A/(4 \times F \times n)$, where j, A, F, and n represent the current density (A cm^{-2}), electrode area, Faraday constant (~ 96485 C mol^{-1}), and the active site density of the catalysts (mole), respectively. It is demonstrated that this amorphous (Ni,Fe)OOH electrode still exhibits a much larger TOF value of 0.073 s^{-1} at 300 mV overpotential, compared to that of the noble IrO_2 and NiFe LDH catalysts (0.0023 s^{-1} and 0.018 s^{-1}, respectively). It is noted that this TOF for the (Ni,Fe)OOH electrode is probably underestimated, considering that not every metal atom is electrochemically active and exposed for the OER, and a small amount of FeOOH is soluble in KOH, but it is enough to confirm the better intrinsic activity of the (Ni,Fe)OOH catalyst than other two catalysts. Its high intrinsic activity may originate from the possible incorporation of Fe cations in solution into NiOOH nanorod arrays, forming $Ni_{1-x}Fe_xOOH$ nanorods with a 30-fold enhancement of the electrical conductivity and improved electronic structures,[29,31-33] which is stable in alkaline electrolyte. Meanwhile, we further extracted the Tafel slopes and exchange current densities of the electrocatalysts (Fig. S9, ESI†) including (Ni,Fe)OOH, IrO_2, and NiFe LDH on Ni foams. It is demonstrated that this (Ni,Fe)OOH catalyst exhibits the lowest Tafel slope (41.5 mV dec^{-1}) and the largest exchange current density (9.9 $\mu A\ cm^{-2}$). After normalization by the active surface area,[34,35] it still has a larger exchange current density than NiFe LDH on Ni foam (Table S2, ESI†). Furthermore, FeOOH itself exhibits very poor electrical conductivity,[20] limiting its electrocatalytic performance. In our case, the predominant compound of conductive NiOOH in the (Ni,Fe)OOH catalyst, strong adhesion between the catalyst and the support, and good conductivity of Ni foam facilitated the charge transfer between the catalyst and the support as highlighted by Fig. S4 (ESI†), which clearly revealed that the charge-transfer resistance of this amorphous electrode (1.29 Ω) is extremely small. These observations demonstrated that the real active sites for the OER may be associated with the porous nanorod arrays of $Ni(OH)_2$-derived amorphous NiOOH mixed with FeOOH on Ni foam, which provides the final catalyst with high intrinsic catalytic activity, high electrochemically active surface area, highly exposed active sites, good electrical conductivity, and fast mass transport pathways.

To go a step further toward industrial applications, it is desirable to investigate full-cell water splitting that converts water to hydrogen at the cathode and oxygen at the anode simultaneously in a two-electrode configuration. Since this amorphous catalyst exhibits a record activity for OER catalysis, it is promising to integrate it with another robust hydrogen evolution reaction (HER) electrocatalyst. Here we paired our new OER electrocatalyst with a $MoNi_4/MoO_2$ cuboid array, a robust non-noble metal-based HER

electrocatalyst (Fig. S10 and S11, ESI†),[19] to make an alkaline electrolyzer in 1 M KOH as plotted in Fig. 4a. The steady-state potential polarization curves of this coupled (Ni,Fe)OOH$^{(+)}$// MoNi$_4$$^{(-)}$ water alkaline electrolyzer are manifested in Figs. 4b and 4c. Impressively, the overall-water-splitting activity of this electrolyzer is far superior to the state-of-the-art IrO$_2$$^{(+)}$//Pt wire$^{(-)}$ coupled electrolyzer. At room temperature, our electrolyzer requires only a cell voltage of 1.464 V to achieve a water-splitting current density of 50 mA cm^{-2}, suggesting ~ 84% electrical-to-fuel efficiency. In particular, this electrolyzer can generate extremely high current densities of 500 and 1,000 mA cm^{-2} at only 1.586 and 1.657 V, respectively, surpassing even the industrial scale (200-400 mA cm^{-2} at 1.8-2.4 V) for hydrogen production, and outperforming the standard Ni and stainless-steel pair used in industrial alkaline electrolyzers by 495 mV and 474 mV at room temperature, respectively. This overpotential difference corresponds to ~ 24% and ~ 22% savings of voltage and energy, respectively. These two values of 1.464 and 1.586 V are record performance indices for overall alkaline water splitting, among the very best inexpensive bifunctional electrocatalysts or heterogeneous catalysts for overall water splitting (Fig. 4d, Fig. 4e, Table S3, ESI†).

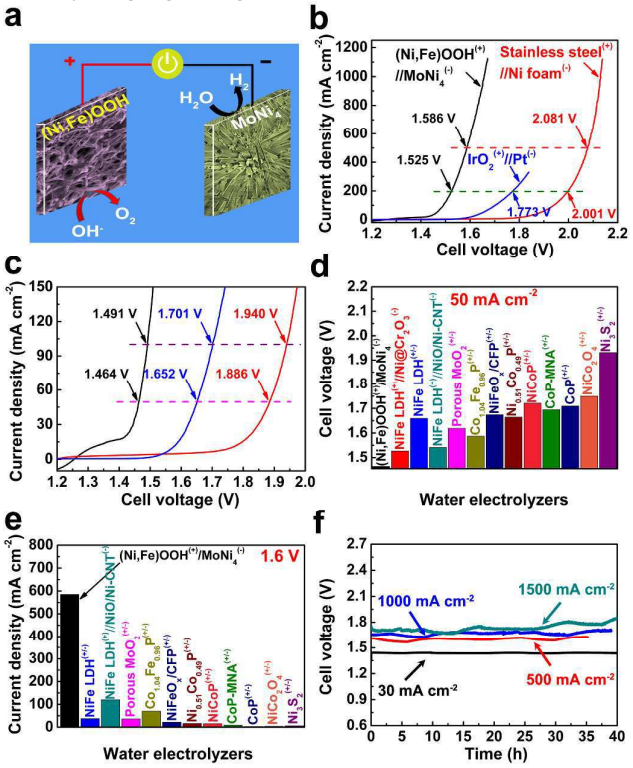

Fig. 4. Overall-water-splitting activity. (a) Diagram showing the construction of an overall-water-splitting electrolyzer with (Ni,Fe)OOH and MoNi$_4$ electrocatalysts as the anode and cathode, respectively. (b,c) Comparison of the overall-water-splitting activities of our designed electrolyzer relative to noble IrO$_2$$^{(+)}$//Pt$^{(-)}$ and stainless steel$^{(+)}$//Ni foam$^{(-)}$ electrolyzers at the (b) high-current and (c) low-current regions. (d) Comparison of the cell voltages at 50 mA cm^{-2} of this electrolyzer with currently available robust electrolyzers in 1M KOH. (e) Comparison of the current densities at a cell voltage of 1.6 V of this electrolyzer with currently available robust electrolyzers in 1M KOH. (f) Durability tests of this electrolyzer at 30, 500, 1,000, and 1,500 mA cm^{-2} in 1M KOH, which clearly show good stability of this electrolyzer when subjected to high-current continuous operation. The symbol "+/-" in Figure 4d and 4e means that both the cathode and anode of this electrolyzer are composed of the same bifunctional catalysts for water splitting.

Electrochemical durability is an important metric to assess the catalytic properties. It is remarkable that this electrolyzer can sustain its outstanding overall-water-splitting performance with no sign of decay for over 40 h when operated at constant current densities of 30, 500, 1,000, and 1,500 mA cm^{-2} (Fig. 4f). To the best of our knowledge, this is the only electrolyzer ever reported to achieve 50 mA cm^{-2} at a voltage of 1.464 V, and to maintain stability at high current densities of 500 and 1,000 mA cm^{-2} at voltages of 1.586 and 1.657 V, respectively, for water electrolysis in a two-electrode configuration. Given its impressive activity, this electrolyzer can be easily promoted by a 1.5 V single-cell AA battery (Fig. S12, ESI†). Additionally, the kinetics and thermodynamics of this electrolyzer can be further boosted by increasing the reaction temperature to 40 ^{o}C, which requires a lower voltage of 1.562 V for 500 mA cm^{-2} (Fig. S13, ESI†), meaning further improvement of its catalytic activity at higher cell temperature as required by industrial use.[3] Finally, the Faradaic efficiency for H_2 and O_2 generation by this electrolyzer was evaluated (Fig. S14, ESI†). We found that H_2 and O_2 gases were the only products from the electrolyzer with their volume ratio close to 2:1, and the efficiency was determined to be nearly 100% during water electrolysis over 1h and beyond. Overall, these electrochemical results imply that our alkaline electrolyzer has great potential to be utilized for scale-up industrial implementation of hydrogen production with high efficiency and low cost.

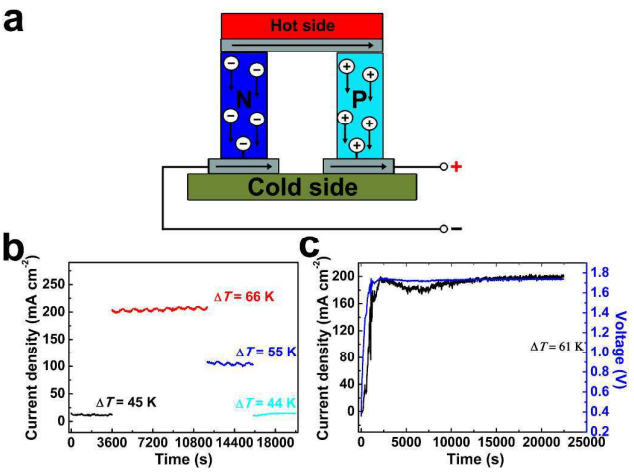

Fig. 5. Overall water splitting driven by a thermoelectric (TE) module. (a) The principle for the power generation between hot and cold sides of a TE module. (b) The real-time dynamics of current densities driven by the power from the TE module when the temperature gradients between hot and cold sides are 45, 66, 55, and 44 K. (c) The real-time stability of the overall water splitting driven by the thermoelectric module when the temperature difference between hot and cold sides is fixed at 61 K.

In addition to the excellent overall-water-splitting activity, we propose to power the electrolyzer using a thermoelectric (TE) module (bismuth telluride) that coverts heat to electricity[36] (Fig. 5a). At present, it is estimated that around 20 to 50% of industrial energy input is turned into waste heat ejected into the surrounding environment. Thus, capturing and storing the abundant waste heat is very attractive for future energy supplies, especially the heat at the low-temperature range (0-120 ^{o}C). In this case, the electrolyzer can efficiently store the waste heat as hydrogen fuel. In Fig. 5b, the temperature gradient between the hot and cold sides is 66 K (87 ^{o}C at the hot side), resulting in a voltage output up to 1.735 V by the TE module. Correspondingly, the electrolyzer is operated stably at a current density as large as 200 mA cm^{-2} (Fig. 5b, c). Even when the temperature gradient across the TE module is reduced to 44 or 45 K, the electrolyzer can still provide 10-15 mA cm^{-2} current density with good stability, implying that we can efficiently convert the waste heat at low temperatures below 100 ^{o}C to produce hydrogen gas.

Conclusions

In conclusion, a robust and durable OER catalyst composed of amorphous interwoven Ni/Fe (oxy)hydroxide nanowire arrays was fabricated at room temperature by a simple method. This OER catalyst requires the lowest overpotentials of 259 and 289 mV to achieve current densities of 500 and 1,000 mA cm^{-2}, respectively, in 1 M KOH with excellent electrochemical durability for over 40 h. Especially, by pairing it with another robust HER catalyst, an outstanding alkaline water electrolyzer was demonstrated with record low voltages of 1.586 and 1.657 V for current densities of 500 and 1,000 mA cm^{-2}, respectively, for overall water splitting, and can be potentially driven by a TE module using waste heat at temperatures below 100 ^{o}C. Our preparation method is simple and safe without any hydrothermal procedures or poisonous materials involved. All of the experiments were performed at room temperature without any high-temperature treatment to save energy, making it very promising and economically viable for large-scale industrial hydrogen production.

Acknowledgements

The work performed at the University of Houston was funded by the US Department of Energy under grant DE-SC0010831, and that in Central China Normal University by the China Scholarship Council, and National Natural Science Foundation of China (Nos. 21377044 and 21573085). H. Z. thanks the supports from Hundred Youth Talents Program of Hunan Province and Xiaoxiang Scholarship from Hunan Normal University. The authors declare no competing financial interests.

References

1 N. S. Lewis and D. G. Nocera, *Proc. Natl. Acad. Sci. USA.*, 2007, **103**, 15729-15735.
2 K. Zeng and D. K. Zhang, *Prog. Energy Combust. Sci.*, 2010, **36**, 307-326.
3 M. Carmo, D. L. Fritz, J. Merge and D. Stolten, *Int. J. Hydrogen Energy*, 2013, **38**, 4901-4934.
4 Y. Sun, M. Delucchi and J. Ogden, *Int. J. Hydrogen Energy*, 2011, **36**, 11116-11127.
5 L. Guo, Z. Yang, K. Marcus, Z. Li, B. Luo, L. Zhou, X. Wang, Y. Du and Y. Yang, *Energy Environ. Sci.*, 2018, **11**, 106-114.
6 H. Y. He, J. H. Lin, W. Fu, X. L. Wang, H. Wang, Q. S. Zeng, Q. Gu, Y. M. Li, C. Yan, B. K. Tay, C. Xue, X. Hu, S. T. Pantelides, W. Zhou and Z. Liu, *Adv. Energy. Mater.* 2016, **6**, 1600464.
7 M. R. Gao, Y. F. Xu, J. Jiang and S. H. Yu, *Chem. Soc. Rev.*, 2013, **42**, 2986-3017.
8 H. Q. Zhou, F. Yu, Y. F. Huang, J. Y. Sun, Z. Zhu, R. J. Nielsen, R. He, J. M. Bao, W. A. Goddard III, S. Chen and Z. F. Ren, *Nat. Commun.*, 2016, 7, 12765.
9 Z. J. Liang and Y. C. Lu, *J. Am. Chem. Soc.*, 2016, **138**, 7574-7583.
10 R. D. L. Smith, M. S. Prévot, R. D. Fagan, Z. P. Zhang, P. A. Sedach, M. K. J. Siu, S. Trudel and C. P. Berlinguette, *Science*, 2013, **340**, 60-63.
11 X. J. Cui, P. J. Ren, D. H. Deng, J. Deng and X. H. Bao, *Energy Environ. Sci.*, 2016, **9**, 123-129.
12 C. C. L. McCrory, S. Jung, J. C. Peters and T. F. Jaramillo, *J. Am. Chem. Soc.*, 2013, **135**, 16977-16987.
13 B. Zhang, et al., *Science*, 2016, **352**, 333-337.
14 F. Yu, H. Q. Zhou, Z. Zhu, J. Y. Sun, R. He, J. M. Bao, S. Chen and Z. F. Ren, *ACS Catal.*, 2017, **7**, 2052-2057.
15 X. Xu, F. Song and X. L. Hu, *Nat. Commun.*, 2016, **7**, 12324.
16 X. G. Wang, W. Li, D. H. Xiong, D. Y. Petrovykh and L. F. Liu, *Adv. Funct. Mater.*, 2016, **20**, 4067-4077.
17 H. Q. Zhou, F. Yu, J. Y. Sun, R. He, S. Chen, C. W. Chu and Z. F. Ren, *Proc. Natl. Acad. Sci. USA.*, 2017, **114**, 5607-5611.
18 Y. Yang, H. L. Fei, G. D. Ruan and J. M. Tour, *Adv. Mater.*, 2015, **27**, 3175-3180.
19 J. Zhang, T. Wang, P. Liu, Z. Q. Liao, S. H. Liu, X. D. Zhuang, M. W. Chen, E. Zschech and X. L. Feng, *Nat. Commun.*, 2017, **8**, 15437.
20 J. X. Feng, H. Xu, Y. T. Dong, S. H. Ye, Y. X. Tong and G. R. Li. *Angew. Chem. Int. Ed.*, 2016, **55**, 3694-3698.
21 H. Q. Zhou, F. Yu, Y. Y. Liu, J. Y. Sun, Z. Zhu, R. He, J. M. Bao, W. A. Goddard III, S. Chen and Z. F. Ren, *Energy Environ. Sci.*, 2017, **10**, 1487-1492.
22 Z. P. Chen, W. C. Ren, L. B. Gao, B. L. Liu, S. F. Pei and H. M. Cheng, *Nat. Mater.*, 2011, **10**, 424-428.
23 J. Q. Liu, M. B. Zheng, X. Q. Shi, H. B. Zeng and H. Xia, *Adv. Funct. Mater.*, 2016, **26**, 919-930.
24 D. Voiry, J. Yang, J. Kupferberg, R. Fullon, C. Lee, H. Y. Jeong, H. S. Shin and M. Chhowalla, *Science*, 2016, **353**, 1413-1416.
25 L. Yu, H. Q. Zhou, J. Y. Sun, F. Qin, F. Yu, J. M. Bao, Y. Yu, S. Chen and Z. F. Ren, *Energy Environ. Sci.*, 2017, **10**, 1820-1827.
26 X. Long, J. K. Li, S. Xiao, K. Y. Yan, Z. L. Wang, H. N. Chen and S. H. Yang, *Angew. Chem. Int. Ed.*, 2014, **53**, 7584-7588.
27 W. D. Chemelewski, H. C. Lee, J. F. Lin, A. J. Bard and C. B. Mullins, *J. Am. Chem. Soc.*, 2014, **136**, 2843-2850.
28 D. L. A. Faria, S. V. Silva and M. T. Oliveira, *J. Raman Spectrosc.*, 1997, **28**, 873-878.
29 M. S. Burke, M. G. Kast, L. Trotochaud, A. M. Smith and S. W. Boettcher, *J. Am. Chem. Soc.*, 2015, **137**, 3638-3648.
30 M. W. Louie and A. T. Bell, *J. Am. Chem. Soc.*, 2013, **135**, 12329-12337.
31 L. Trotochaud, S. L. Young, J. K. Ranney and S. W. Boettcher, *J. Am. Chem. Soc.*, 2014, **136**, 6744-6753.
32 M. B. Stevens, C. D. M. Trang, L. J. Enman, J. Deng and S. W. Boettcher, *J. Am. Chem. Soc.*, 2017, **139**, 11361-11364.
33 D. Friebel, M. W. Louie, M. Bajdich, K. E. Sanwald, Y. Cai, A. M. Wise, M. Cheng, D. Sokaras, T. Weng, R. Alonso-Mori, R. C.

Davis, J. R. Bargar, J. K. Nørskov, A Nilsson and A. T. Bell, *J. Am. Chem. Soc.*, 2015, **137**, 1305-1313.

34 M. C. Acevedo, M. L. Stone, J. R. Schmidt, J. G. Thomas, Q. Ding, H. C. Chang, M. L. Tsai, J. H. He and S. Jin, *Nat. Mater.,* 2015, **14**, 1245-1251.

35 I. K. Mishra, H. Q. Zhou, J. Y. Sun, K. Dahal, Z. S. Ren, R. He, S. Chen and Z. F. Ren. *Mater. Today Phys*., 2018, **4**, 1-6.

36 F. J. DiSalvo, *Science*, 1999, **285**, 703-706.

Energy & Environmental Science

Paper

The table of contents entry

A robust oxygen-evolving electrocatalyst was developped by a room-temperature strategy for water splitting at high current densities with low voltages.

TOC figure